RESEARCH ARTICLE

Editorial Process: Submission:02/12/2019 Acceptance:08/08/2019

Nannochloropsis Extract–Mediated Synthesis of Biogenic Silver Nanoparticles, Characterization and *In Vitro* Assessment of Antimicrobial, Antioxidant and Cytotoxic Activities

Princely Ebenezer Gnanakani[1,2], Perumal Santhanam[3], Kumpati Premkumar[4], Kilari Eswar Kumar[5], Magharla Dasaratha Dhanaraju[2]*

Abstract

Objective: To investigate the biogenic synthesis of silver nanoparticles (AgNPs) using partially purified ethyl acetate extract of *Nannochloropsis* sp. hexane (EAENH) fraction of microalga. **Methods:** The green synthesis of AgNPs was confirmed with UV-Vis spectrum which shows the surface plasmon resonance (SPR) at 421 nm. Fourier Transform Infrared Spectra (FTIR) presented the involvement of functional groups like carboxyl groups of fatty acids, tetraterpenoids of xanthophylls, hydroxyl groups of polyphenols, carbonyl and amide linkage of proteins in the AgNP synthesis. Gas Chromatography-Mass Spectrometry analysis (GCMS) revealed that phytochemicals like octadecanoic acid and hexadecanoic acid imply in capping, bioreduction, and stabilization of AgNps. **Result:** High-resolution Transmission electron microscope (HRTEM), Dynamic light scattering (DLS), X-ray diffraction (XRD) and EDX analysis showed the crystalline form of the AgNPs with Z-average size 57.25 nm. The zeta potential value of -25.7 mV demonstrated the negative surface charge and colloidal stability of AgNPs. The antimicrobial activity of AgNPs displayed effective inhibition zone against selected bacterial and fungal pathogens. In vitro, antioxidant effects were assessed by 1,1-diphenyl-2-picryl-hydrazyl (DPPH), hydrogen peroxide and reducing power assays which revealed excellent scavenging potential for AgNPs than the extracts. The anti-proliferative potential of biofabricated AgNPs and extracts on Human Non-small lung cancer cell line (A549) was assessed using 3–(4,5-dimethylthiazol-2-yl)-2,5-diphenyl-tetrazolium bromide (MTT) assay with IC_{50} values of 15 µgmL-1 and 175 µgmL-1 respectively. **Conclusion:** The study reveals that the microalgae-mediated AgNPs possesses potent antimicrobial and antioxidant activity along with the ability to stimulate apoptosis in A-549 cell line.

Keywords: *Nannochloropsis*- silver nanoparticles-antioxidant activity- cytotoxic activity

Asian Pac J Cancer Prev, **20 (8)**, 2353-2364

Introduction

Cancer is one of the leading causes of death accounting for 9.6 million deaths worldwide annually (Bray et al., 2018). Lung cancer is the most common cause of cancer deaths with about 1.7 million deaths per year, having a poor prognosis (Murray, 2016). At present chemotherapy, radiotherapy and surgery are used for cancer therapy, which is capable of destroying both the normal and cancer cells producing unwanted adverse effects thus weakening the immune system (Rao et al., 2016). To overcome this challenge, it is prudent to formulate a drug that is safe, non-toxic, eco-friendly, biocompatible and cost-effective for cancer therapy that is selectively toxic to cancer cells with less or no side effects. Thus, the discovery of new natural cytotoxic agents has, therefore, become a key global strategy in preventing cancer (El-Baz et al., 2014). The application of nano-biotechnology plays an important role in the development of nanomedicine as an alternative and effective therapy for cancer (Barabadi et al., 2017).

Recently, biofabricated nanoparticle synthesis from plants and microbial sources has become an evolving strategy in the nanomedicine due to their eco-friendly, inexpensive and less toxic nature (Borase et al., 2014). The green NPs are recognized as valuable therapeutic agents since they have a unique size with crystalline form (1–100 nm), larger surface area to volume ratio, drug encapsulation, biocompatibility and thermal conductivity (Moteriya and Chanda, 2017). The bionanomaterial synthesis involves metals like gold, silver, iron, zinc, titanium, and copper produced from various bio-sources as stated (Borase et al., 2014). Nanoparticle research is

*[1]Department of Pharmaceutical Biotechnology, Research Scholar, JNTUK, [2]Department of Pharmaceutical Sciences, Research Director, GIET School of Pharmacy, Rajahmundry, [5]Department of Pharmacology, AU College of Pharmaceutical Sciences, Andhra University, Vishakhapatnam, Andhra Pradesh, [3]Department of Marine Science, [4]Department of Biomedical Science, Bharathidasan University, Tiruchirappalli, Tamilnadu, India. *For Correspondence: mddhanaraju@yahoo.com*

presently a topic of interest for scientific investigation due to an extensive diversity with potential applications in pharmaceutical, biomedical, diagnostics, cosmetic, environmental and electronic fields (Singh et al., 2016). Several products acquired from algae have great demand in biological research due to its synergistic action of phytochemicals. Also, some biological organisms like seaweeds, plants, and microbes have been explored for the synthesis of NPs (Ramanathan et al., 2011). The biosynthesized nanoparticles from marine microorganisms are exceedingly valuable in therapeutics, compared to the native metal NPs, as these biosynthesized NPs are rich in biochemicals like flavonoids, fatty acids, oxygenated terpenoids, saponins, polysaccharides, polyphenols, proteins, attributed to their considerable antioxidant efficacy (Chokshi et al., 2016)

Reactive oxygen species (ROS) produced by the incomplete reduction of oxygen are distributed as by-products for metabolic cellular reactions in the body. Lower ROS concentrations are essential for cellular activities such as cell progression, intracellular signaling, and cell defense. On the contrary, higher ROS concentrations proficiently lead to oxidative stress which causes direct or indirect ROS-regulated damage of proteins, nucleic acids, and lipids. It was, therefore, acknowledged that taking antioxidant supplements regularly in our diet could combat intimidating diseases, especially cancer (Rajendran et al., 2017). The extracts with higher scavenging capacity are more influential in the production of biogenic AgNPs (Vahid et al.,2014)

In this study, the microalgae *Nannochloropsis* sp. (NC) a green alga belonging to eustigmatophyceae class and chlorophyceae group has been selected. It comprises phytochemicals like fatty acids, terpenoids, xanthophylls, polyphenols and lower volume of proteins which have effective antibacterial, anti-inflammatory, immunomodulatory, antioxidant and cytotoxic properties. The baseline information for microalgae mediated NPs is still scarce and further attempts for bio-prospecting of algae are emphasized for several therapeutic applications. There is a paucity of reports on the biosynthesis of microalgae-mediated metallic nanoparticles with antibacterial, antioxidant and anticancer properties (Ali et al., 2011). This paper validates a green approach for the biogenic synthesis of AgNPs using the partially purified EAENH fractions following characterization studies. The antimicrobial, antioxidant and cytotoxic effects of AgNPs on the human non-small lung cancer cell line (A549) have subsequently been assessed.

Materials and Methods

Materials

EAENH fractionated powder obtained was stored at 4°C from the antioxidant screening studies. Silver nitrate (AgNO3), DPPH, potassium ferricyanide, trichloroacetic acid, l-ascorbic acid, and 3–(4,5-dimethylthiazol-2-yl)-2,5-diphenyl-tetrazolium bromide (MTT) were purchased from Sigma Aldrich (Mumbai, India). Nutrient broth, Mueller Hinton agar and ferric chloride were acquired from SD Fine Chemicals Limited, (Mumbai, India). Dulbecco's modified eagle medium (DMEM) and fetal bovine serum (FBS) were bought from MolychemPvt. Ltd. (Mumbai, India). Human non-small lung cancer cell line (A549) was procured from NCCS Pune, India and utilized. Any other chemicals used were of analytical grades.

Preparation of Nannochloropsis sp. Extraction

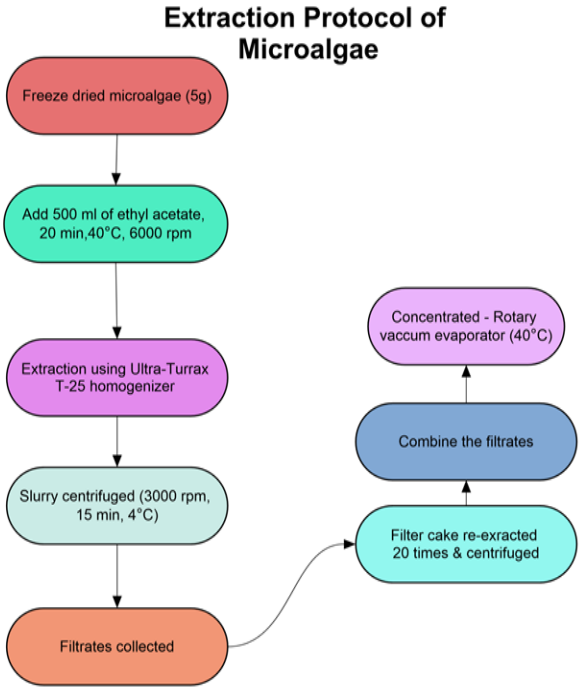

The biomass dry weight was noticed to be 5 g. The percentage yield of ethyl acetate extract was 38.88% (1.9 g). The dried ethyl acetate extract was stored in an airtight glass container for further investigation. The resulting extract was partially purified further using an open silica column chromatography; eluted with mixture of hexane: ethyl acetate, ethyl acetate: methanol and toluene: ethyl acetate; active fractions collected using TLC; evaporated resulting in a concentrated thick residue i.e., EAENH powder (Gnanakani et al., 2019).

P*reparation of Aqueous Extract of Nannochloropsis sp.*

One gram of EAENH powder was mixed with 100 mL of deionized water in a water bath at 60°C for 10 min and then filtered through Whatman filter paper (Grade 1). The filtrate was stored at 4°C for further evaluation studies.

Biosynthesis of AgNPs

The synthesis of nanoparticles was carried out in a sterile conical flask, by adding 10 ml of the aqueous extract and 90 ml of 1 mM aqueous $AgNO_3$ solution. Besides, 100 ml of 1 mM aqueous Silver nitrate $AgNO_3$ solution was kept as control. The mixtures were incubated for seven days at 60°C, however, when the temperature was increased to 80°C, the particle formation also increases. AgNPs formation was observed by a visual color change from light green to dark brown by reducing Ag^+ to Ag^0 (Packia Lekshmi et al., 2012). The solution was centrifuged for 25 min at 4°C at 16,000 rpm. Then the supernatant was removed to eliminate unreacted silver ions and the dark brown pellet settled at the bottom of the tube.

The pellet was separated and purified from the mixture by washing with sterile distilled water and then lyophilized using LY00555 LYODEL Freeze dryer. The lyophilized AgNPs were stored at 4°C for further investigations.

Nanocharacterization of biosynthesized AgNPs

The bioreduction of silver ions in aqueous mixtures of *Nannochloropsis* was examined by a UV-visible spectrophotometer, at the wavelength of 200 – 700 nm using Shimandzu model SL-210 (Shah et al., 2018). In DLS analysis, the particle size and zeta potential of the AgNPs were evaluated by a Zetasizer (Horiba Scientific NanoPartica Nanoparticle Analyzer SZ-100) operated at 37°C (Raja et al., 2017). The XRD analysis for the biosynthesized AgNPs were performed in a Bruker Kappa APEXII instrument in the 2Ɵ range of 30 - 80°C (Chahardoli et al., 2017). The FTIR spectrum was recorded in the mid-infrared region (4,000–400 cm^{-1}) at room resolution (Shimadzu IR spectrophotometer, model 840, Japan) to detect the phytochemicals accountable for the bioreduction of AgNPs (Elshawy et al., 2016). The TEM analysis was performed using a JEOL 3010 instrument to detect the size and shape of the particles. The elemental composition of the biogenic AgNPs was determined by EDX analysis (Kattarath and Ramani, 2017).

GCMS analysis of EAENH

GCMS analysis of EAENH fraction was performed using a Shimadzu/ QP2020GC instrument coupled with MS-5975 inert MSD and triple axis mass selective ion detector. The identification of phytochemicals was achieved using the National Institute Standard and Technology MS library (NIST- MS library) database (Heidari et al., 2018).

Antimicrobial activity - Well diffusion assay

The antimicrobial activity of biosynthesized AgNPs was assessed by agar well diffusion method. Gram-negative (Pseudomonas aeruginosa and Escherichia coli), Gram-positive bacteria (Staphylococcus aureus and Bacillus subtilis) and fungi (Candida albicans and Aspergillus niger) were obtained from the Department of Microbiology, GSL Institute of Medical Science, Rajahmundry, India. Mueller-Hinton (MH) broth and Sabouraud dextrose broth were used to cultivate bacterial and fungal pathogens respectively. The strains were inoculated on the MH agar plate, then wells were formed at 6 mm in diameter. The concentration of 10, 20 and 30 µL of the AgNPs (1 mg mL^{-1}) and EAENH (1 mg mL^{-1}) was loaded to the wells and incubated at 37°C for 24 h. The antibiotics cefotaxime (1 mg mL^{-1}) was employed as the standard for comparison on each agar plate. The inhibition zone was measured for AgNPs and EAENH (Gomaa, 2017). The experiment was performed in triplicates.

DPPH (1,1-diphenyl-2-picryl-hydrazyl) free radical scavenging assay

DPPH assay for EAENH and its biosynthesized AgNPs was analysed (Venkatesan et al., 2016). The concentration ranges of 20 – 100 µg/mL of the samples were used (ascorbic acid used as standard). The percentage inhibition was calculated using the formula

$$\% \text{ inhibition} = [(A_0-A_1)/A_0] \times 100$$

Where A_0 is the absorbance of the control; A_1 is the absorbance of the sample.

Ascorbic acid was used as a reference or testing agent attributed to the ease of use and reliability (O'Sullivan et al., 2011; Ahmed et al., 2015).

Hydrogen peroxide radical scavenging assay

Hydrogen peroxide assay of the EAENH and its biosynthesized AgNPs was performed (Kumar et al., 2016). In this assay, different concentrations (20 - 100 µg/mL) of the samples were used, and ascorbic acid was utilized as standard. The percentage of scavenging activity was calculated using the following formula:

$$\% \text{ scavenging activity} = [(A_0-A_1)/A_0] \times 100$$

Where A_0 is the absorbance of the control; A_1 is the absorbance of the sample.

Reducing power assay

The ferric reducing power of the EAENH and its biosynthesized AgNPs were determined (Alavi and Karimi, 2017). The concentrations were used in the range of 20 – 100 µg/mL and the standard used as ascorbic acid. Based on the absorbance value, the ferric reducing power was expressed. IC_{50} values were calculated using the linear regression curve for all the antioxidant assays.

In vitro cytotoxicity assay

Cell viability test was performed using the MTT assay (Vijayan et al., 2018). Human Non-Small lung cancer cell line (A-549) was cultivated with DMEM media with 10% FBS, and antibiotic mixture (penicillin, ampicillin and streptomycin 100 Units/mL) maintained at 37°C, 5% CO_2 and 95% humidity. The cells were added into a 96-well plate at the density of 2×10^4 per well. After incubation at 37°C for 24 h, the cells were treated with EAENH fractions (200 – 20 µg/mL) and biosynthesized AgNPs (2 – 20 µg/mL) by serial dilution with Dimethyl sulfoxide (DMSO) and Cisplatin drug as standard (0.1 g/mL). The A-549 cells were trypsinised and counted using hemocytometer. Then 100 µl of A-549 cells were added to the poly L-lysine coated 96-well plate, incubated at 37°C in 5% CO_2 incubator. After 24 h incubation, the old medium was replenished with fresh medium and 50 µl of EAENH fraction and AgNPs solution were added and incubated for 48 h at 37°C in 5% CO_2 incubator. Then 30 µl of 0.5% w/v MTT was added and incubated for 4 h at 37°C. Add 50 µl of acidic-isopropanol after incubation to dissolve the formazan formed and incubated for 30 minutes at 37°C. Then absorbance was observed at 554 using a microplate reader. The experiments were carried out in triplicates and the half-inhibitory concentration (IC_{50}) was estimated graphically using graph pad prism software.

The percentage of cell viability was calculated using

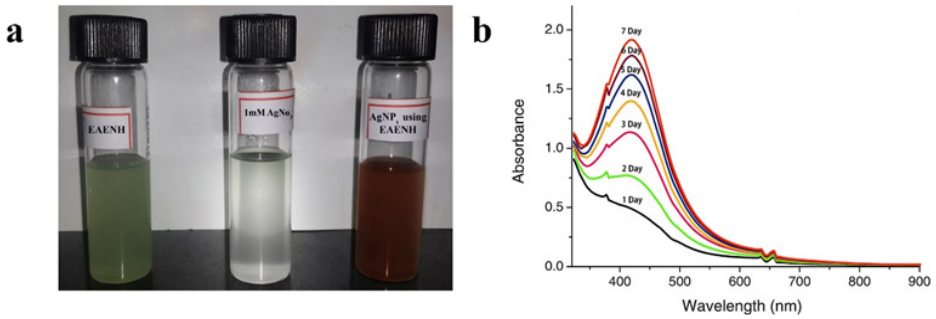

Figure 1. Biosynthesis of AgNPs. a, Biogenic synthesis of Silver nanoparticles using Ethyl acetate extract *Nannochloropsis* hexane fraction; b, Ultraviolet – Visible absorption spectrum of biosynthesized Silver nanoparticles using Ethyl acetate extract *Nannochloropsis* hexane fraction.

the formula:

$$\% \text{ Cell Viability} = [\text{Abs (sample)} / \text{Abs (control)}] \times 100.$$

Apoptosis analysis - Hoechst Staining

The IC_{50} concentrations of the EAENH and AgNPs derived EAENH were treated with A-549 cells ($1x10^5$ cells per well) and Hoechst staining was performed to know the apoptosis level (Dehghanizade et al., 2017). A-549 cells were added into six-well plates at 3×10^5 cells per well, incubated at 37°C for 24 h. It was further treated with EAENH and AgNPs at IC_{50} concentrations and again incubated for 4 h. The Hoechst 33342 staining assay was employed to examine morphological alterations of the cells (Yamakawa et al., 2008).

DNA fragmentation test

The A-549 cells (1×10^6) had been treated with sardine oil for 48 h and grown in specific 100 mm plates. The cells were rinsed with PBS at pH 7.5, centrifuged at 12,000 rpm for harvest at 4°C and sediment was collected. The separated sediment was incubated with DNA lysis buffer [1mM EDTA, 10 nMTris pH (7.5), 400 mM NaCl, and 1%Triton X-100] for 30 min followed by centrifugation. The supernatant was collected and further incubated with RNase overnight at 37°C (0.2 mg/ml) followed by proteinase K (0.1 mg/ml) at 37°C for 2 h. The DNA was separated using phenol, chloroform, and isoamyl alcohol (25:24:1) amalgam; precipitated using sodium acetate and absolute ethanol. Then the equivalent quantity of sample DNA (20 µg) was electrophoresed using agarose gel (1.5%) in Tris-borate EDTA buffer followed by ethidium bromide staining. The fragmented DNA was pictured utilizing ultraviolet light (Bethu et al., 2018).

Statistical Analysis

The data were statistically evaluated using GraphPad prism (Windows version 6.01, GraphPad Software, La Jolla, California, USA) for linear regression. Statistical analysis was performed using SPSS version16 software (SPSS Inc., Chicago, IL) and the results were evaluated by one way ANOVA and Tukey's test. Values were presented as mean ± S.D. of the three replicates of each experiment. The results with $p < 0.05$ were considered to be statistically significant.

Results

Characterization of EAENH-AgNPs

The biosynthesis of AgNPs using EAENH fractionated powder was successfully formed when incubated with 1 mM AgNO3 solution (Figure 1a). The absorbance and the peak intensity of the colloidal solution were observed at 421 nm using UV–Vis spectrophotometer. The UV-Vis absorbance spectra were documented for the extract with 1 mM AgNO3 solution at various time intervals (0, 1, 2, 3, 4, 5, 6 and 7 days) (Figure 1b). The color becomes darker with an increase in the incubation time from light green to light brown and finally reddish-brown until ten days as a result of the excitation of SPR which evidences the formation of AgNPs with unique optical properties (Abdel-Aziz et al., 2014). TEM analysis presented the size details and confirmed the size and shape of biosynthesized AgNPs (Figure 2). They were polydispersed and predominantly spherical, cubical and hexagonal shaped with a mean average size of 57.25 nm.

The DLS analysis was used to determine particle size and its distribution of nanoparticles which specifies maximum intensity at 57.25 nm with a size range of 8 -137 nm (Figure 3a). The polydispersity index (PDI) of AgNPs was found to be 0.364 which showed that the synthesized particles were polydispersed. Zeta potential was related to the electrophoretic mobility and stability of the colloidal suspension of AgNPs. Negative zeta potential of about -25.7 mV confirmed high energy barrier, ideal surface

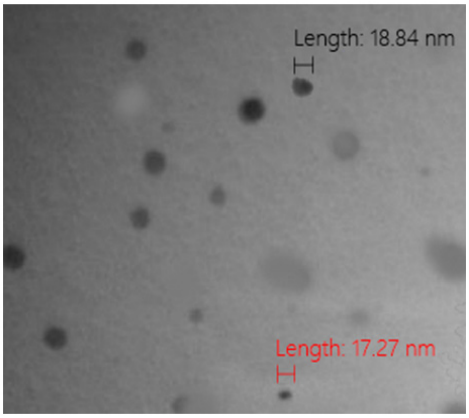

Figure 2. Transmission Electron Micrograph of Biosynthesized Silver Nanoparticles Using Ethyl Acetate Extract *Nannochloropsis* Hexane Fraction.

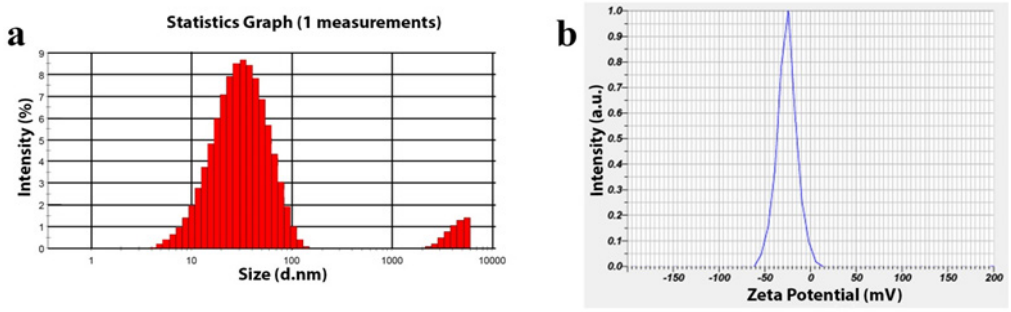

Figure 3. Particle Size Analysis. a, Dynamic Light Scattering analysis of biosynthesized Silver nanoparticles using Ethyl acetate extract *Nannochloropsis* hexane fraction; b, Zeta potential of biosynthesized Silver nanoparticles using Ethyl acetate extract *Nannochloropsis* hexane fraction

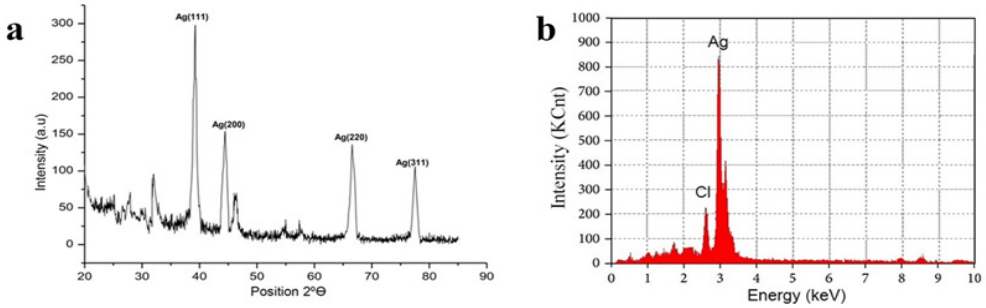

Figure 4. Crystal Analysis of AgNPs. a, X-ray Diffraction analysis of biosynthesized Silver nanoparticles using Ethyl acetate extract *Nannochloropsis* hexane fraction; b, Energy Dispersive X-ray spectroscopy analysis of biosynthesized Silver nanoparticles using Ethyl acetate extract *Nannochloropsis* hexane fraction

charge, and repulsion amongst particles which establish the stability of the particles (Figure 3b).

The crystalline nature of synthesized AgNPs was confirmed by XRD analysis. The pattern exhibits four prominent Bragg's reflection with 2Θ values at about 38.2, 44.7, 64.2, 77.3 which assign to (111), (200), (220) and (321) facets of the face-centred cubic (fcc) crystal structure respectively confirming the biosynthesis of AgNPs (Yugandhar and Savithramma, 2016) as shown (Figure 4a). The EDX spectrum showed an intense peak of 2.981 KeV authenticating the existence of elemental silver in NPs, confirmed by the elementary mapping of AgNPs with silver mapped in red (Figure 4b).

FTIR analysis

FTIR analysis was performed to identify the potential biochemical accountable for the reduction of silver ions and capping of AgNPs. The FTIR spectrum obtained for the biosynthesized AgNPs (Figure 5a) and EAENH fraction (Figure 5b) was illustrated. For EAENH fraction, the peak at 3,435 cm^{-1} was due to the –OH stretching, $–NH^{3+}$ stretching and N–H stretching of amide band,

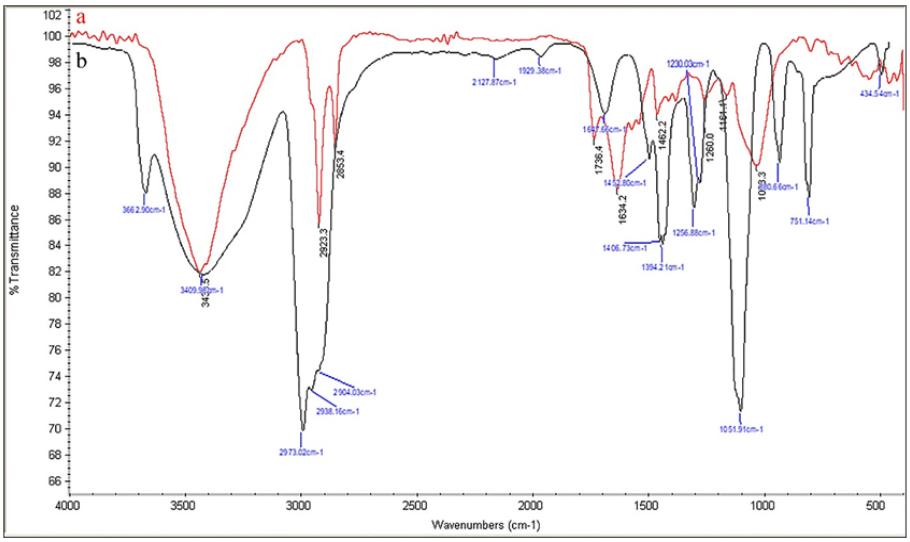

Figure 5. FT-IR Spectral Analysis. a, Biosynthesized Silver nanoparticles using Ethyl acetate extract *Nannochloropsis* hexane fraction; b, Ethyl acetate extract *Nannochloropsis* hexane fraction.

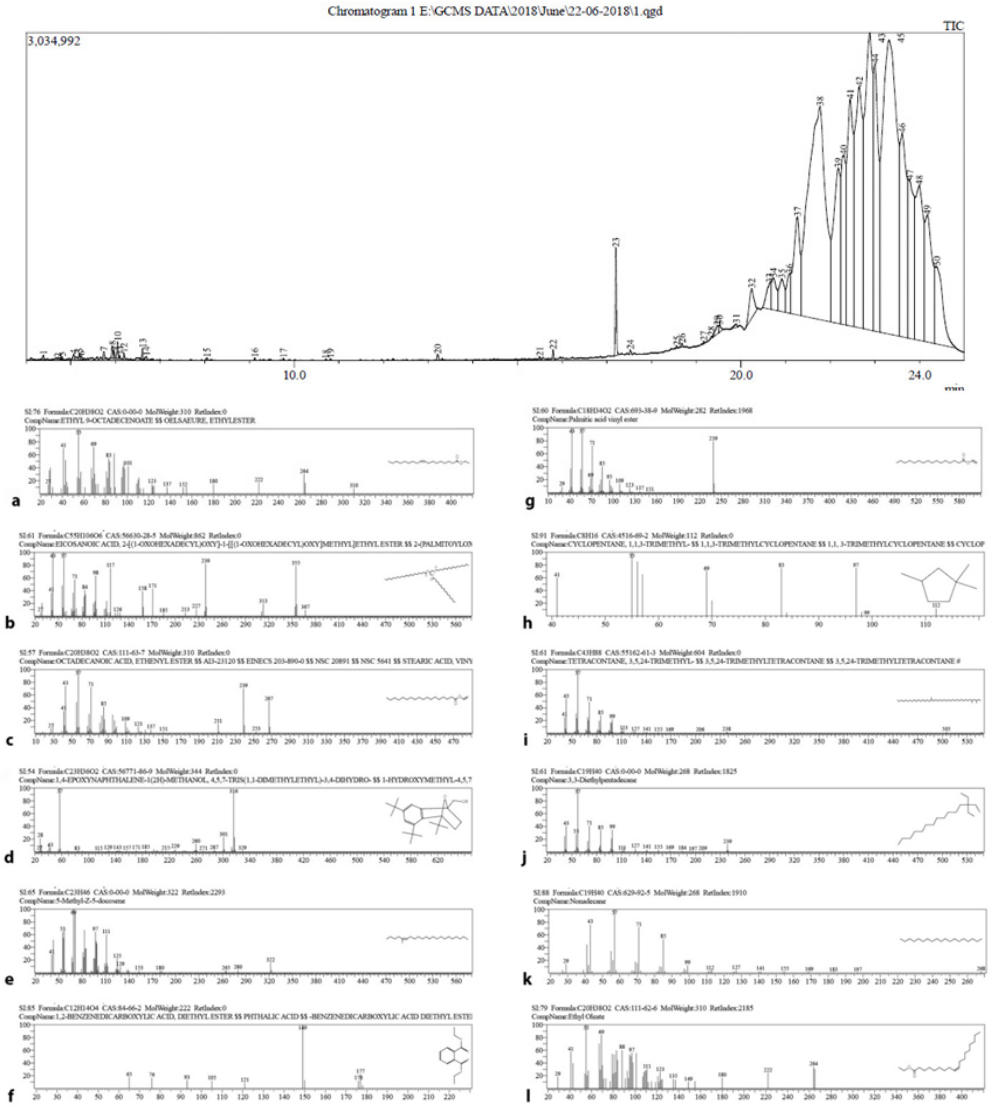

Figure 6. Gas Chromatography – Mass Spectroscopy and Structure of Bioactive Phytochemicals Identified in the Ethyl Acetate Extract *Nannochloropsis* Hexane Fraction. a, "Ethyl 9-Octadecenoate" at retention time 21.77 and Hit 2; b, "Eicosanoic acid, 2-[(1-oxohexadecyl)oxy]-1-[[(1-oxohexadecyl)oxy]methyl] ethyl ester" at retention time 23.3 and Hit 5 ;c, "Octadecanoic acid, ethenyl ester" at retention time 24.17 and Hit 1; d, "1,4-epoxynaphthalene-1 (2H)-methanol, 4,5,7-tris (1,1-dimethylethyl)-3,4–dihydro-" at retention time 21.08 and Hit 2; e, "5-Methyl-Z-5-docosene" at retention time 20.73 and Hit 4.; f, "1,2-Benzenedicarboxylic acid, diethyl ester" at retention time 13.21 and Hit 1; g, "Palmitic acid vinyl ester" at retention time 24.38 and Hit 3; h, "1,1,3-Trimethyl cyclopentane" at retention time 7.63 and Hit 2; i, "3,5,24-Trimethyl tetracontane" at retention time 11.96 and Hit 3; j, "3,3-Diethylpentadecane" at retention time 9.49 and Hit 5; k, "Nonadecane" at retention time 5.97 and Hit 1; l, "Ethyl Oleate" at retention time 19.17 and Hit 1.

which shows the presence of proteins, carbohydrates, and lipids that indicate participation in silver ion reduction. An intense band at 2,923 cm^{-1} was due to CH3 stretching and strong N–H stretch which showed the presence of lipids and proteins. A sharp band at 2,853 cm^{-1} was due to CH_2 and N–H stretching of the Amide band of protein, which indicates that the bands were related to lipids and proteins. The weak intense band 1,736 cm^{-1} and a sharp peak at 1,634 cm^{-1} were due to C–O stretching of fatty acid esters and C=O stretching of amides indicating the presence of fatty acids and conjugated ketones respectively. A sharp dominant peak observed at 1,161 cm^{-1} was due to C–O–C stretching which signified the presence of carbohydrates. An intense peak was found at 1,033 cm^{-1} due to O–H stretching of flavonoids or phenol.

GCMS analysis of Nannochloropsis-extracts

The GCMS analysis predominant constituents of the EAENH fraction were Octadecanoic acid (10.9%) followed by Hexadecanoic acid (8.32%), Octadecanoic acid, ethenyl ester (6.87%) 1, 4 - epoxynaphthalene - 1 (2H) - methanol, 4,5,7-tris (1,1 - dimethylethyl) - 3,4 – dihydro - (7.1%), 5-Methyl-Z-5-docosene (3.24%), 1,2-Benzenedicarboxylic acid (5.61%) and 1,2-Cyclopentanediol (4.81%). Nearly thirty compounds were present in traces (Figure 6).

Antimicrobial activity

In this study, the antimicrobial activity of EAENH fraction and its biosynthesized AgNPs were assessed against six clinical pathogenic organisms including *E.*

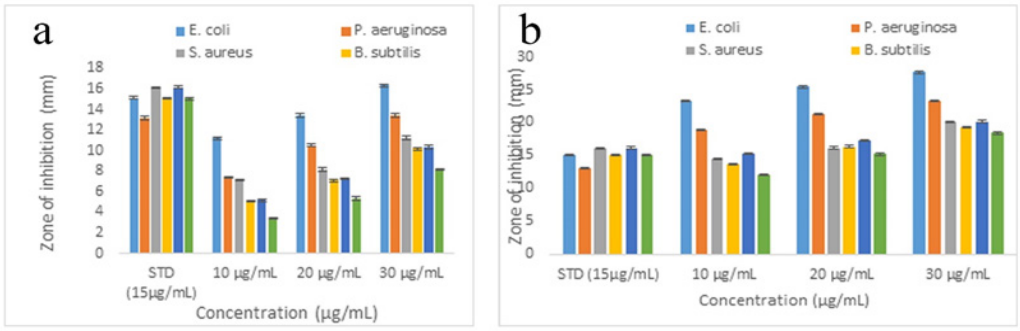

Figure 7. Antimicrobial Assay. a, Ethyl acetate extract *Nannochloropsis* hexane fraction; b, Biosynthesized Silver nanoparticles.

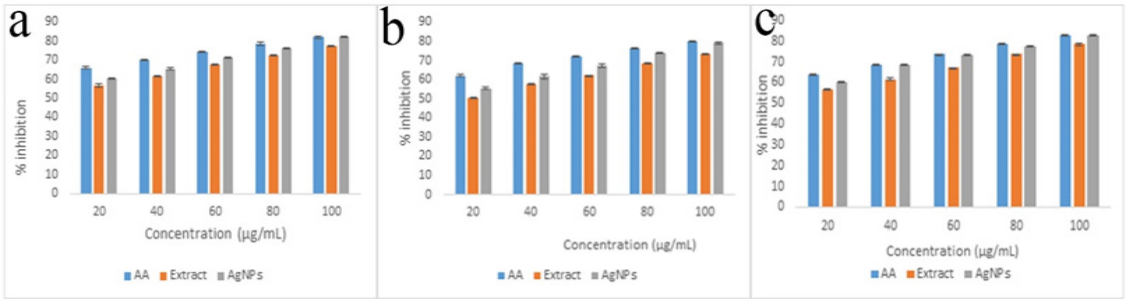

Figure 8. Antioxidant Activity of Ethyl Acetate Extract *Nannochloropsis* Hexane and Biosynthesized Silver Nanoparticles Using Ethyl Acetate Extract *Nannochloropsis* Hexane Fraction. a, 1,1-diphenyl-2-picryl-hydrazyl assay; b, Hydrogen peroxide assay, (c) Reducing power assay.

coli, *P. aeruginosa*, *S. aureus*, *B. subtilis*, *C. albicans*, and *A. niger*. The reports revealed broad-spectrum antimicrobial efficiency which differed in inhibition against selected pathogens. The zone of inhibition diameter was observed, each well loaded with EAENH (Figure 7a) and AgNPs as shown (Figure 7b). Hence, by increasing the concentration of the fractions and AgNPs from 10 to 30 µl, the inhibition diameter increases for all tested pathogens which illustrates dose-dependent activity. The maximum inhibition zone was found against *E. coli* (16.33 mm for EAENH and 27.61 mm for AgNPs), *P. aeruginosa* (13.41 mm for EAENH and 23.25 mm for AgNPs) and *C. albicans* (10.32 mm for EAENH and 20.15 mm for AgNPs).

Antioxidant activity

The antioxidant potential was examined to know whether the scavenging effects of the fraction increased or decreased after nanoparticle synthesis. The DPPH (Figure 8a), hydrogen peroxide (Figure 8b) and reducing power (Figure 8c) assays were conducted to detect the presence of capped antioxidants in the AgNPs and their potential was compared using ascorbic acid as standard. The antioxidant assays of both the EAENH and AgNPs increased in a dose-dependent manner and significant activity was noticeable for AgNPs when compared to the fraction. The DPPH, HPA and FRAP IC_{50} values of AgNPs were found to be 11.28, 16.03 and 11.04 µg/ml, respectively; whereas for EAENH fraction, it was observed to be 13.9, 21.22 and 14.58 µg/ml respectively.

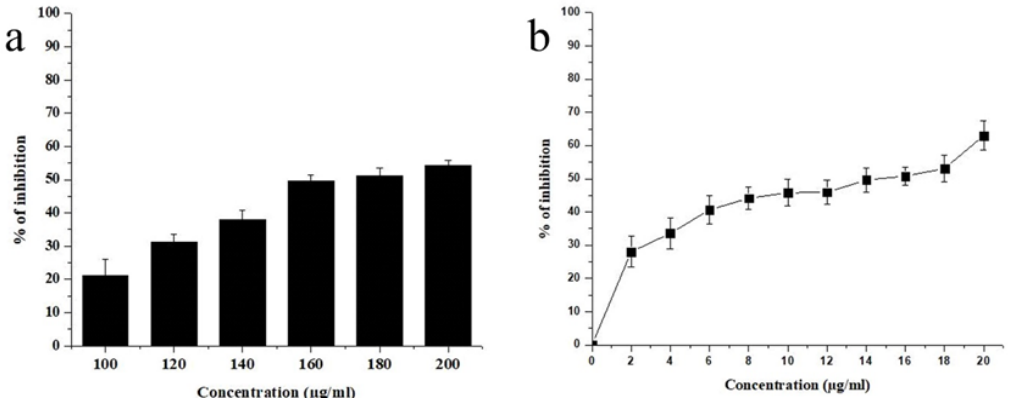

Figure 9. Cell Viability Assay (3–(4,5-dimethylthiazol-2-yl)-2,5-diphenyl-tetrazolium Bromide Assay). a, Ethyl acetate extract *Nannochloropsis* hexane fraction, (b) Biosynthesized Silver nanoparticles using Ethyl acetate extract *Nannochloropsis* hexane fraction.

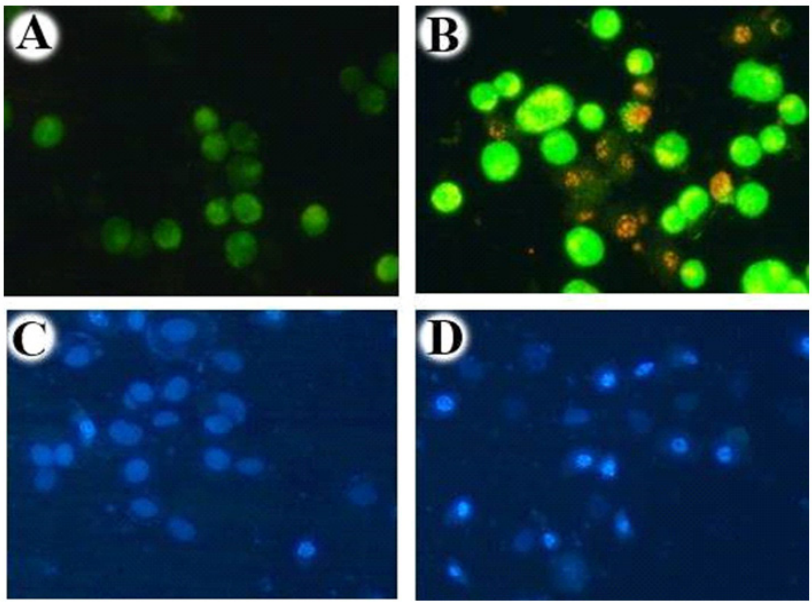

Figure 10. Acridine Orange/Ethidium Bromide and Hoechst Staining of Ethyl Acetate Extract *Nannochloropsis* hexane. To differentiate live and dead cells based on their morphological features, treated and untreated cells were stained with Acridine orange/Ethidium bromide, Hoechst and visualised using fluorescent microscopy. A, Acridine orange/Ethidium bromide staining of untreated cells displayed green nuclei with an intact nuclear architecture; B, Acridine orange/Ethidium bromide staining of Ethyl acetate extract *Nannochloropsis* hexane fraction treated cells displayed green and red nuclei with cell shrinkage, nuclear condensation; C, Hoechst staining of untreated cells; D, Hoechst staining of Ethyl acetate extract *Nannochloropsis* hexane fraction treated cells. This result strongly demonstrates that the IC_{50} concentration (175 µg/ml) of extracted fraction hold the ability to induce apoptosis in the Human Non-small lung cancer cell line (A549).

Cytotoxic potential

Due to their lower adverse effects, the exploration of therapeutic anticancer agents from marine resources has increased in the past decade. The phytochemicals possessing antioxidant potential might have anti-proliferative properties since they have the ability

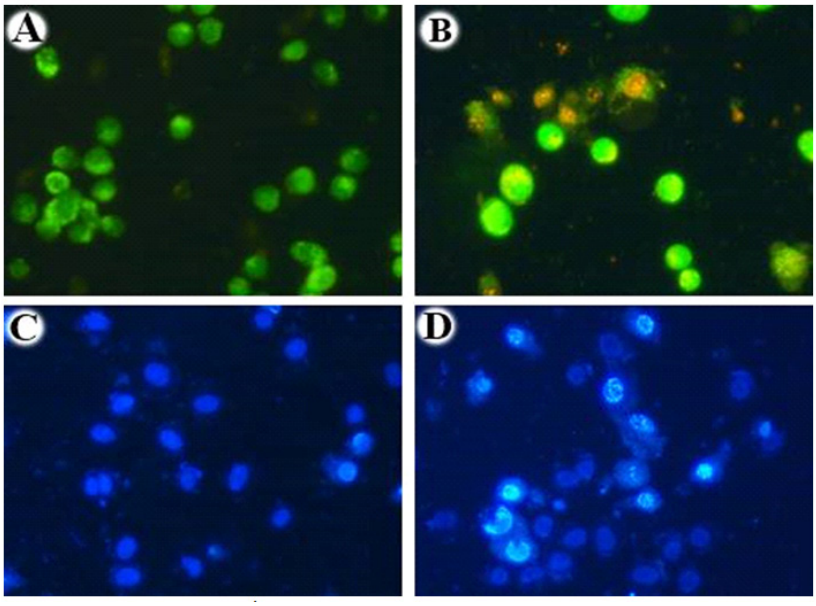

Figure 11. Acridine Orange/Ethidium Bromide and Hoechst Staining of Biosynthesized Silver Nanoparticles Using Ethyl Acetate Extract *Nannochloropsis* Hexane Fraction. To differentiate live and dead cells based on their morphological features, treated and untreated cells were stained with Acridine orange/Ethidium bromide, Hoechst and visualised using fluorescent microscopy. A, Acridine orange/Ethidium bromide staining of untreated cells displayed green nuclei with an intact nuclear architecture (control); B, Acridine orange/Ethidium bromide staining of the Silver Nanoparticle treated cells displayed green and red nuclei with cell shrinkage, nuclear condensation; C, Hoechst staining of untreated cells with intact nuclear architecture (control); D, Hoechst staining of Ethyl acetate extract *Nannochloropsis* hexane fraction treated cells displayed nuclei with cell shrinkage, nuclear condensation. This result strongly demonstrates that the IC_{50} concentration (15 µg/ml) of Silver Nanoparticle hold the ability to induce apoptosis in the Human Non-small lung cancer cell line (A549).

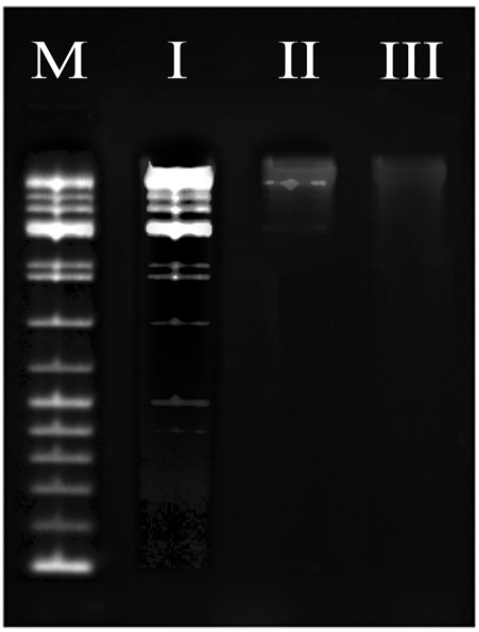

Figure 12. Evaluation of Apoptotic activity of Ethyl Acetate Extract *Nannochloropsis* Hexane Fraction and Silver Nanoparticles Mediated EAENH by Deoxyribonucleic Acid fragmentation Assay; Lane M, Deoxyribonucleic acid marker; Lane I, control (untreated cells with 0.5% Dimethyl Sulfoxide), Lane II, cells treated with EAENH microalgal fraction at IC_{50} concentration (175 µg/ml); Lane III, cells treated with Silver nanoparticles using Ethyl acetate extract *Nannochloropsis* hexane fraction at IC_{50} concentration (15 µg/ml)

to obstruct the activity of unusually expressing signaling proteins. The anticancer activity of the EAENH and biosynthesized AgNPs was investigated using the Human Non-Small lung cancer cell line (A-549). The standard was observed to be statistically significant ($p<0.05$). The reports revealed that the A-549 cell proliferation was extensively inhibited by AgNPs (Figure 9b) with an IC_{50} value of 15 μgmL^{-1} while EAENH (Figure 9a) showed 175 μgmL^{-1} respectively as shown. The cell toxicity of both EAENH fraction and AgNPs were dose-dependent and nanoparticles showed significant cytotoxicity compared to the fraction. Previous reports indicated the dose-dependent cytotoxicity of biogenic AgNPs on cancer cell lines (Gliga et al., 2018).

Apoptotic study of cancer cells treated with Nannochloropsis-AgNPs

The apoptotic effect of EAENH (Figure 10) and biosynthesized AgNPs (Figure 11) were examined on A-549 cells stained with Hoechst 33258 for 48 h. In this study, after the treatment with IC_{50} concentrations of EAENH and AgNPs for 48 h, A-549 cells present nuclear fragmentation, cell shrinkage and plasma membrane blebbing. These morphological alterations influence apoptotic cell death.

DNA fragmentation

This test established that the EAENH IC_{50} concentration treated with A-549 cells (Lane II) and AgNPs IC_{50} concentration treated A-549 cells (Lane III) represented double-strand breakage, thus generating a ladder form, whereas control A-549 cells treated with DMSO (Lane I) exhibited minimum breakage (Lane I) (Figure 12).

Discussion

The rapid extracellular synthesis suggested the procedure to be inexpensive, eco-friendly and simple for downstream processing feasible for large-scale production of AgNPs. The change in color during AgNPs formation was directly related to the concentration of EAENH and temperature, which may well be attributed to the reducing agents such as saponins, tetraterpenoids, flavonoids, sterols, polyphenols, and peptides. The observed broad plasmon band shows that the particles were polydispersed due to its size distribution. A previous study with green algae showed the absorption range of AgNPs at a peak of 420 and 436 nm by *C. vulgaris* and *C. calcitrans* correspondingly (Panneerselvam et al., 2015). Earlier findings revealed the biosynthesis of AgNPs, with a size range of 8-20 nm using Chlorella vulgaris (Xie et al., 2007). The size evaluated in the DLS technique was the hydrodynamic diameter of the theoretical area which disperses with the same speed as of the evaluated nanoparticles. Thus, the size determined in the DLS technique was usually broader in contrast with TEM analysis as confirmed by other researchers (Nayak et al., 2016). The high zeta potential value indicated a wide-spread electrical charge on the surface of the particles, which might produce intense repellent force between particles to control agglomeration (Lin et al., 2008). The weak signals in XRD presented along with the silver showed the presence of oxygen, carbon, hydrogen, phosphorus and nitrogen elements, which signified the confirmation of extracellular biochemical moieties capped onto the metal surface of the NPs correlating well with the previous literature (Selvam et al., 2017). The previous investigation for the optimization and characterization of AgNPs using microalgae *Isochrysis galbana* in EDX proved this required metal phase (Ranjitham et al., 2013).

For biogenic AgNPs, it was found that a shift occurred in the FTIR absorbance from 2,853 to 2,973 cm^{-1} when compared to EAENH fraction. Furthermore, the substantial decrease in band strength was noticed from 1,647 to 1,634 cm^{-1}. This difference indicated the association of these bands in the AgNPs production. The appearance of an extra band at 1,736 cm^{-1} suggests the reduction of Ag^{+} due to the oxidation of polyphenolic groups. Also, a shift in the peaks of AgNPs from 1,647, 1,230 and 1,051 cm^{-1} to 1,634, 1,161 and 1,033 cm^{-1} respectively were evidenced. The fresh peaks in the fingerprint zone (1,736 and 1,260 cm^{-1}) validated functional groups conversion during AgNPs synthesis. Thus, FTIR analysis clearly specified that the carboxyl groups of fatty acids, tetraterpenoids of xanthophylls, carboxyl and hydroxyl groups of polyphenols, carbonyl and amide linkage of proteins might be actively involved in the formation of biosynthesized AgNPs. In addition, related work involved hydroxyl and amino protein groups in the biosynthesis of AgNPs from the *Chlorella vulgaris* microalgae extract (Annamalai and Nallamuthu, 2016). GCMS analysis concludes that the

phytochemicals like octadecanoic acid, hexadecanoic acid, oxygenated tetraterpenoids and phenolic acids present in EAENH fraction were accountable for bioreduction and stabilization of AgNPs.

For the antimicrobial effect, the variations in the activity for bacteria could be attributed to the entry of silver ions through outer membrane proteins of gram-negative by effectively creating pits thereby altering its permeability and thick peptidoglycan layer of gram-positive which play a major role in protecting the cells from penetration of AgNPs into the cell wall providing less antibacterial effect (Li et al., 2010). Similarly, AgNPs fabricate ROS which induced oxidative stress and lysed the microbial cells by denaturing proteins or damaging the DNA (Roy et al., 2019). Previous studies displayed that highly reactive metal oxide nanoparticles show tremendous biocidal activity against gram-positive and gram-negative bacteria (Yousefzadi et al., 2014). A similar antioxidant study showed the dose-dependent increase in DPPH scavenging by biosynthesized AgNPs using the plant *Helicteres isora* root extract (Bhakya et al., 2016). Hence, AgNPs could be employed as a potent antioxidant agent.

For microalgae, a dearth of reports was available on the cytotoxic effects of biosynthesized AgNPs against cell lines. The probable cytotoxic mechanism was due to the disruption of the gene involved in the regulation of cell cycle and oxidative degradation of lipids with AgNPs which also induces DNA denaturation, necrosis, and apoptosis in cancer cells. A similar study using algal species Microcystis aeruginosa was performed and cytotoxic potentialities were due to the release of phytochemicals and silver ions (Ag^+) from the particle surface (El-Sheekh and El-Kassas, 2014). In apoptosis, membrane blebbing was considered to be the foremost morphological alteration of cells regulated by the interaction of caspase substrate cleavage (Dehghanizade et al., 2017). These results suggested that apoptosis induction by EAENH and AgNPs-mediated EAENH fraction confirmed its direct anti-cancer effect. Fragmented DNA was attributed to the induction of apoptosis in A-549 cells (Gurunathan et al., 2014). Altogether, these results afford in vitro proofs for the anticancer efficacy of the EAENH and biosynthesized AgNPs using EAENH for the successful use of colloidal drugs as an anticancer agent.

In conclusion, the reports of this study propose that stable AgNPs have been successfully synthesized using the bioactive molecules present in the EAENH fraction as reducing and capping agents with its promising reports which proved to be a good start for further exploration. The AgNPs exhibited a potent antimicrobial effect against *E. coli*, *P. aeruginosa*, and *C. albican*s than the fraction. The investigations revealed efficient antioxidant and cytotoxic activity even at low concentrations for AgNPs compared to the fraction. The significant cytotoxicity could be due to the synergistic effect of the biomolecules, silver ions and increased oxidative stress which induces apoptosis. For future studies, *in vivo* and physiological barriers should be investigated to effectively deliver nanoparticles into the cancer cells. The green nanocarriers will be an interesting area for researchers in chemotherapeutics due to its site-specific delivery. This work established that biogenic AgNPs using *Nannochloropsis* sp. exhibit satisfactory physical parameters and biological activities which might serve as a promising nano-drug against A-549 cell line and selected pathogen.

Acknowledgements

This study is not financially supported by any grant agency or government institution. This research work is approved by Institutional Ethics Committee (IEC), Bharathidasan University, Tiruchirappalli, Tamilnadu, India. This work is part of an approved PhD thesis work. The authors declare that there is no financial association or other potential conflicts of interest. There is no conflict of ethical issues for this work. The authors are thankful to Management, GIET School of Pharmacy; Department of Marine Science and Biomedical Science, Bharathidasan University, Tiruchirappalli, Tamilnadu, India for providing their kind support. We also thank Mrs. Regina Rajkumar for her English review.

Conflict of interest

The authors declare that there is no financial associations or other potential conflicts of interest.

References

Abdel-Aziz MS, Shaheen MS, El-Nekeety AA, Abdel-Wahhab MA (2014). Antioxidant and antibacterial activity of silver nanoparticles biosynthesized u'poosing Chenopodium murale leaf extract. *J Saudi Chem Soc*, **18**, 356–63.

Abdel-Raouf N, Alharbi RM, Al-Enazi NM, Alkhulaifi MM, Ibraheem IBM (2017). Rapid biosynthesis of silver nanoparticles using the marine red alga Laurencia catarinensis and their characterization. *Beni-Suef Univ J Basic Appl Sci*, **7**, 150-7.

Ahmed D, Khan M, Saeed R (2015). Comparative analysis of phenolics, flavonoids, and antioxidant and antibacterial potential of methanolic, hexanic and aqueous extracts from adiantum caudatum leaves. *Antioxidants*, **4**, 394–409.

Alavi M, Karimi N (2017). Characterization, antibacterial, total antioxidant, scavenging, reducing power and ion chelating activities of green synthesized silver, copper and titanium dioxide nanoparticles using Artemisia haussknechtii leaf extract. *Artif Cells Nanomedicine Biotechnol*, **46**, 2066-81.

Ali DM, Sasikala M, Gunasekaran M, Thajuddin N (2011). Biosynthesis and characterization of silver nanoparticles using marine cyanobacterium, Oscillatoria willei NTDM01. *Dig J Nanomater Biostructures*, **6**, 385–90.

Annamalai J, Nallamuthu T (2016). Green synthesis of silver nanoparticles: characterization and determination of antibacterial potency. *Appl Nanosci***, 6**, 259–65.

Asmathunisha N, Kathiresan K (2013). A review on biosynthesis of nanoparticles by marine organisms. *Colloids Surfaces B Biointerfaces*, **103**, 283–7.

Barabadi H, Ovais M, Shinwari ZK, Saravanan M (2017). Anti-cancer green bionanomaterials: present status and future prospects. *Green Chem Lett Rev*, **10**, 285–314.

Bethu MS, Netala VR, Domdi L, Tartte V, Janapala VR (2018). Potential anticancer activity of biogenic silver nanoparticles using leaf extract of Rhynchosia suaveolens: an insight into the mechanism. *Artif Cells Nanomedicine Biotechnol*, **46**,

104-14.
Bhakya S, Muthukrishnan S, Sukumaran M, Muthukumar M (2016). Biogenic synthesis of silver nanoparticles and their antioxidant and antibacterial activity. *Appl Nanosci*, **6**, 755–66.
Borase HP, Salunke BK, Salunkhe RB, et al (2014). Plant extract: A promising biomatrix for ecofriendly, controlled synthesis of silver nanoparticles. *Appl Biochem Biotechnol*, **173**, 1–29.
Bray F, Ferlay J, Soerjomataram I, et al (2018). Global cancer statistics 2018: GLOBOCAN estimates of incidence and mortality worldwide for 36 cancers in 185 countries. *CA Cancer J Clin*, **68**, 394–424.
Chahardoli A, Karimi N, Fattahi A (2017). Biosynthesis, characterization, antimicrobial and cytotoxic effects of silver nanoparticles using nigella arvensis seed extract. *Iran J Pharm Res*, **16**, 1167–75.
Chokshi K, Pancha I, Ghosh T, et al (2016). Green synthesis, characterization and antioxidant potential of silver nanoparticles biosynthesized from de-oiled biomass of thermotolerant oleaginous microalgae Acutodesmus dimorphus. *RSC Adv*, **6**, 72269–74.
Dehghanizade S, Arasteh J, Mirzaie A (2017). Green synthesis of silver nanoparticles using Anthemis atropatana extract: characterization and in vitro biological activities. *Artif Cells Nanomedicine Biotechnol*, **46**, 160-8.
El-Baz FK, El-Baroty GS, Ibrahim AE, El-Baky HHA (2014). Cytotoxicity, antioxidants and antimicrobial activities of lipids extracted from some Marine Algae. *J Aquac Res Dev*, **5**, 284–8.
El-Sheekh MM, El-Kassas HY (2014). Application of biosynthesized silver nanoparticles against a cancer promoter cyanobacterium, Microcystis aeruginosa. *Asian Pac J Cancer Prev*, **15**, 6773–9.
Elshawy OE, Helmy EA, Rashed LA (2016). Evaluation of the antitumor activity of the biologically synthesized silver nanoparticles. *Adv Nanoparticles*, **5**, 149–66.
Gliga AR, Di Bucchianico S, Lindvall J, Fadeel B, Karlsson HL (2018). RNA-sequencing reveals long-term effects of silver nanoparticles on human lung cells. *Sci Rep*, **8**, 1–14.
Gomaa EZ (2017). Antimicrobial, antioxidant and antitumor activities of silver nanoparticles synthesized by Allium cepa extract: A green approach. *J Genet Eng Biotechnol*, **15**, 49–57.
Goodarzi V, Zamani H, Bajuli L, Moradshahi A (2014). Evaluation of antioxidant potential and reduction capacity of some plant extracts in silver nanoparticles' synthesis. *Mol Biol Res Commun*, **3**, 165–74.
Gurunathan S, Han J, Eppakayala V, Jeyaraj M, Kim J-H (2014). Cytotoxicity of biologically synthesized silver nanoparticles in MDA-MB-231 human breast cancer cells. *Beilstein J Nanotechnol*, **5**, 1590–602.
Heidari Z, Salehzadeh A, Ataollah S, Shandiz S, Tajdoost S (2018). Anticancer and antioxidant properties of ethanolic leaf extract of Thymus vulgaris and its bio-functionalized silver nanoparticles. *Biotech*, **8**, 1–14.
Jayaraman T, Arumugam Raja S, Priya A, Jagannathan M, Ashokkumar M (2015). Synthesis of a visible-light active V2O5-g-C3N4 heterojunction as an efficient photocatalytic and photoelectrochemical material. *New J Chem*, **39**, 1367–74.
Kattarath SS, D GR (2017). Bioproduction and characterization of silver nanoparticles from microalgae Asteracys quadricellulares, its antimicrobial and antibiofilm activities. *Int J Pharma Biosci*, **8**, 714–25.
Khalil T, Raza A, Shinwari ZK (2016). Green synthesis of silver nanoparticles via plant extracts : beginning a new era in cancer theranostics. *Nanomedicine (Lond)*, **11**, 3157–77.
Kumar B, Smita K, Seqqat R, et al (2016). In vitro evaluation of silver nanoparticles cytotoxicity on Hepatic cancer (Hep-G2) cell line and their antioxidant activity: Green approach for fabrication and application. *J Photochem Photobiol B Biol*, **159**, 8–13.
Li WR, Xie XB, Shi QS, et al (2010). Antibacterial activity and mechanism of silver nanoparticles on Escherichia coli. *Appl Microbiol Biotechnol*, **85**, 1115–22.
Lin L, Qiu P, Cao X, Jin L (2008). Colloidal silver nanoparticles modified electrode and its application to the electroanalysis of Cytochrome c. *Electrochim Acta*, **53**, 5368–72.
Madhanraj R, Eyini M, Balaji P (2017). Antioxidant assay of gold and silver nanoparticles from edible basidiomycetes mushroom fungi. *Free Radicals Antioxidants*, **7**, 137–42.
Moteriya P, Chanda S (2017). Synthesis and characterization of silver nanoparticles using Caesalpinia pulcherrima flower extract and assessment of their in vitro antimicrobial, antioxidant, cytotoxic, and genotoxic activities. *Artif Cells Nanomedicine Biotechnol*, **45**, 1556–67.
Murray CJL (2016). Global, regional, and national comparative risk assessment of 79 behavioural, environmental and occupational, and metabolic risks or clusters of risks, 1990–2015: a systematic analysis for the Global Burden of Disease Study 2015. *Lancet*, **388**, 1659–724.
Nayak D, Ashe S, Rauta PR, Kumari M, Nayak B (2016). Bark extract mediated green synthesis of silver nanoparticles: Evaluation of antimicrobial activity and antiproliferative response against osteosarcoma. *Mater Sci Eng C*, **58**, 44–52.
O'Sullivan AM, O'Callaghan YC, O'Grady MN, et al (2011). In vitro and cellular antioxidant activities of seaweed extracts prepared from five brown seaweeds harvested in spring from the west coast of Ireland. *Food Chem*, **126**, 1064–70.
Packia Lekshmi NC, Sumi SB, Viveka S, Jeeva S, Raja Brindha J (2012). Antibacterial activity of nanoparticles from *Allium sp*. *J Microbiol Biotechnol Res*, **2**, 115–9.
Panneerselvam K, Mohan D, Abishek G, Priya R (2015). Synthesis of silver nanoparticles using Phytoplankton and its characteristics. *Int J Fish Aquat Stud*, **2**, 398–401.
Raja S, Ramesh V, Thivaharan V (2017). Green biosynthesis of silver nanoparticles using Calliandra haematocephala leaf extract, their antibacterial activity and hydrogen peroxide sensing capability. *Arab J Chem*, **10**, 253–61.
Ramanathan R, O'Mullane AP, Parikh RY, et al (2011). Bacterial kinetics-controlled shape-directed biosynthesis of silver nanoplates using Morganella psychrotolerans. *Langmuir*, **27**, 714–9.
Ranjitham AM, Suja R, Caroling G, Tiwari S (2013). In vitro evaluation of antioxidant, antimicrobial, anticancer activities and characterisation of *Brassica Oleracea. var. bortrytis. L* synthesized silver nanoparticles. *Int J Pharm Pharm Sci*, **5**, 239–51.
Rao PV, Nallappan D, Madhavi K, et al (2016). Phytochemicals and biogenic metallic nanoparticles as anticancer agents. *Oxid Med Cell Longev*, **5**, 1–15.
Roy A, Bulut O, Some S, Mandal AK, Yilmaz MD (2019). Green synthesis of silver nanoparticles: biomolecule-nanoparticle organizations targeting antimicrobial activity. *RSC Adv*, **9**, 2673-702.
Selvam K, Sudhakar C, Govarthanan M, et al (2017). Eco-friendly biosynthesis and characterization of silver nanoparticles using Tinospora cordifolia (Thunb.) Miers and evaluate its antibacterial, antioxidant potential. *J Radiat Res Appl Sci*, **10**, 6–12.
Shah Z, Aftab A, Sikandar K, et al (2018). Biogenic synthesis of silver nanoparticles using extracts of Leptolyngbya JSC-1 that induce apoptosis in HeLa cell line and exterminate pathogenic bacteria. *Artif Cells Nanomedicine Biotechnol*,

46, 471-80.
Singh P, Kim YJ, Wang C, Mathiyalagan R, Yang DC (2016). The development of a green approach for the biosynthesis of silver and gold nanoparticles by using Panax ginseng root extract, and their biological applications. *Artif Cells Nanomedicine Biotechnol*, **44**, 1150–7.
Venkatesan J, Kim S-K, Shim M (2016). Antimicrobial, Antioxidant, and Anticancer Activities of Biosynthesized Silver Nanoparticles Using Marine Algae Ecklonia cava. *Nanomaterials*, **6**, 1–18.
Vijayan R, Joseph S, Mathew B (2018). Indigofera tinctoria leaf extract mediated green synthesis of silver and gold nanoparticles and assessment of their anticancer, antimicrobial, antioxidant and catalytic properties. *Artif Cells Nanomedicine Biotechnol*, **46**, 861–71.
Xie J, Lee JY, Wang DIC, Ting YP (2007). Silver nanoplates: From biological to biomimetic synthesis. *ACS Nano*, **1**, 429–39.
Yamakawa S, Demizu A, Kawaratani Y, et al (2008). Growth inhibition of human colon cancer cell line HCT116 by bis [2-(acylamino)phenyl] disulfide and its action mechanism. *Biol Pharm Bull*, **31**, 916–20.
Yousefzadi M, Rahimi Z, Ghafori V (2014). The green synthesis, characterization and antimicrobial activities of silver nanoparticles synthesized from green alga Enteromorpha flexuosa (wulfen). *J Agardh Mater Lett*, **137**, 1–4.
Yugandhar P, Savithramma N (2016). Biosynthesis, characterization and antimicrobial studies of green synthesized silver nanoparticles from fruit extract of Syzygium alternifolium (Wt.) Walp. an endemic, endangered medicinal tree taxon. *Appl Nanosci*, **6**, 223–33.